Available online at www.sciencedirect.com
SCIENCE DIRECT®
Chemical Physics Letters 382 (2003) 567–572
CHEMICAL PHYSICS LETTERS
www.elsevier.com/locate/cplett

Electron field emission from fluorinated amorphous carbon nanoparticles on porous alumina

S.H. Lai [a], K.P. Huang [b], Y.M. Pan [a], Y.L. Chen [a], L.H. Chan [a], P. Lin [b], H.C. Shih [a,*]

[a] *Department of Materials Science and Engineering, National Tsing Hua University, 101, Sec. 2, Kuang Fu Road, Hsinchu, Taiwan 300, ROC*

[b] *Department of Materials Science and Engineering, National Chiao Tung University, 1001 Ta Hsueh Road, Hsinchu, Taiwan 300, ROC*

Received 27 August 2003; in final form 16 October 2003

Abstract

The fluorinated amorphous carbon nanoparticles (a-C:F NPs) films have been prepared on a *porous alumina* at a lower temperature of ~100 °C by an *ECR-CVD* system with a mixture of CF_4, C_2H_2 and Ar as precursors. The morphology of a-C:F NPs films was verified by *FESEM*. The microstructure and chemical bonding nature of the a-C:F NPs films were investigated by Raman spectroscopy and *XPS*, respectively. *The fluorinated samples* need a lower field (~2.25 V/μm for 10.6% F a-C:F NPs films) to emit the electron than unfluorinated ones. The excellent field-emission properties of a-C:F NPs films are due to the effect of the shape, fluorine doping and dangling bonds.

1. Introduction

Carbon-based materials are one of the most well-known materials to human life and they are available with a variety of properties. Various carbon-based materials such as chemical vapor deposited (CVD) diamond [1], diamond-like carbon (DLC) films [2] and carbon nanotubes (CNTs) [3,4] have proven to be very interesting electron-emitting cathodes because of their excellent electron field-emission properties. The CNTs seem to be the best field emitters among all carbon-based materials owing to their high aspect ratios, high chemical stability, and high mechanic strength. It is believed that the lower work function (compared with Si, Mo, and W materials) and field-enhancement effect are the main reasons for the low turn-on voltage and high current density of the CNTs. Compared to CNTs, carbon nanoparticles have their advantages, such as the ball shape and lower synthesis temperatures, for field-emission materials [5]. A porous alumina (PA) has recently attracted increasing attention as a key material for the fabrication of nanodevices [6–8]. In this Letter, fluorinated amorphous carbon nanoparticles (a-C:F

* Corresponding author. Fax: +886-35-710290.
E-mail address: hcshih@mse.nthu.edu.tw (H.C. Shih).

0009-2614/$ - see front matter © 2003 Elsevier B.V. All rights reserved.
doi:10.1016/j.cplett.2003.10.106

NPs) films have been prepared on a PA template at a lower temperature of ~100 °C by an electron cyclotron resonance chemical vapor deposition (ECR-CVD) system and the field-emission properties of the film also have been investigated.

2. Experimental

A commercially available membrane filter, 13 mm o.d. and 60 μm thick (Whatman Ltd., Anodisc 13), which consists of an array of tubular channels with a diameter of about 100 nm as a template. The ECR-CVD system used in this work has been described elsewhere [9,10]. The experimental conditions for the deposition of a-C:F NPs are as follows: a microwave power of 800 W, a total gas pressure of 5×10^{-3} Torr, CF_4 flow rate of 5–20 sccm, C_2H_2 flow rate of 10–20 sccm, and Ar flow rate of 10–20 sccm for 1 min under a r.f. bias of 100–200 V. The morphology of the sample was observed by field-emission scanning electron microscopy (FESEM; JEOL JSM-6300F). The chemical bonding of the a-C:F NPs films was investigated by X-ray photoelectron spectroscopy (XPS Perkin–Elmer Model PHI1600 system) using a single Mg Kα (1253.6 eV) X-ray source operating at 250 W. Energy calibration was made by reference to the Au $4f_{7/2}$ peak at 83.8 eV. The channel width was 1.0 eV for survey scan spectra and 0.2 eV for core-level spectra. The film microstructure was also analyzed by Raman spectroscopy (Ranishaw Ramanscope Model 2001), whose excitation was achieved by means of the 514.4 nm (2.41 eV) line of an argon ion (Ar^+) laser (Coherent Innovr Model 90). The electron field-emission characteristics of a-C:F NPs films were measured by the conventional diode method in the vacuum chamber with 10^{-5} Torr pressure. The current density and the electric field (J–E) characteristics were measured using an electrometer (Keithley 237). The field-emission measurements were carried out using a parallel plate structure with the films being the cathode and an indium-tin-oxide (ITO) coated glass as the anode. The gap between the cathode and the anode was 200 μm by a glass fiber spacer. The results are reproducible over periods of weeks and the emission properties of a-C:F NPs films do not degrade with the exposure to atmospheric conditions.

3. Results and discussion

The top surface of the PA template, directly exposed to the ECR plasma, was coated with a-C:F NPs films after completion of the experiment. Fig. 1(a) is a typical SEM top-view micrograph of the deposited films, which shows the nanostructures of the a-C:F NPs. The large particles are deposited on the interpore of PA and then the small particles are formed among the large particles. Although the size of the a-C:F NPs is not uniform (<100 nm), the small particles are distributed uniformly all over the films. Fig. 1(b) gives the cross-sectional view of the mono-layer a-C:F NPs on the PA template. The smaller particles were also observed in the tubular channels. It should be noted that the a-C:F NPs are irregular balls and the particle surface is ragged. Besides, the a-C:F NPs film was synthesized under several experimental parameters, such as microwave power, gas flow rate, and a r.f. bias. We tried to increase the F content, but instead of nanoparticles, other morphologies were produced, i.e., the highest F content of the a-C:F NPs is 10.6 at.%. The dense, flat and covered films were formed on the porous alumina in most experimental parameters. Other morphologies are the nanowires in and the nanoporous films on the porous alumina, and they will be discussed in another Letter.

The growth mechanism of a-C:F NPs film was proposed as shown in Figs. 1(c) and (d). Initially, the plasma stream of the ion fluxes is guided to the PA template by a r.f. bias and the a-C:F NPs are deposited on the interpore and nanochannels of PA template due to the agglomeration of CF_x radicals. As the deposited time increasing, a-C:F NPs are growing bigger and smaller a-C:F NPs are also produced among the bigger ones. Besides the growth process of a-C:F NPs, the etching process also proceed by the plasma at the same time. Finally, a-C:F NPs film is deposited on the PA template.

Fig. 2 shows the C 1s and F 1s spectra of the a-C:F NPs film with three different fluorine con-

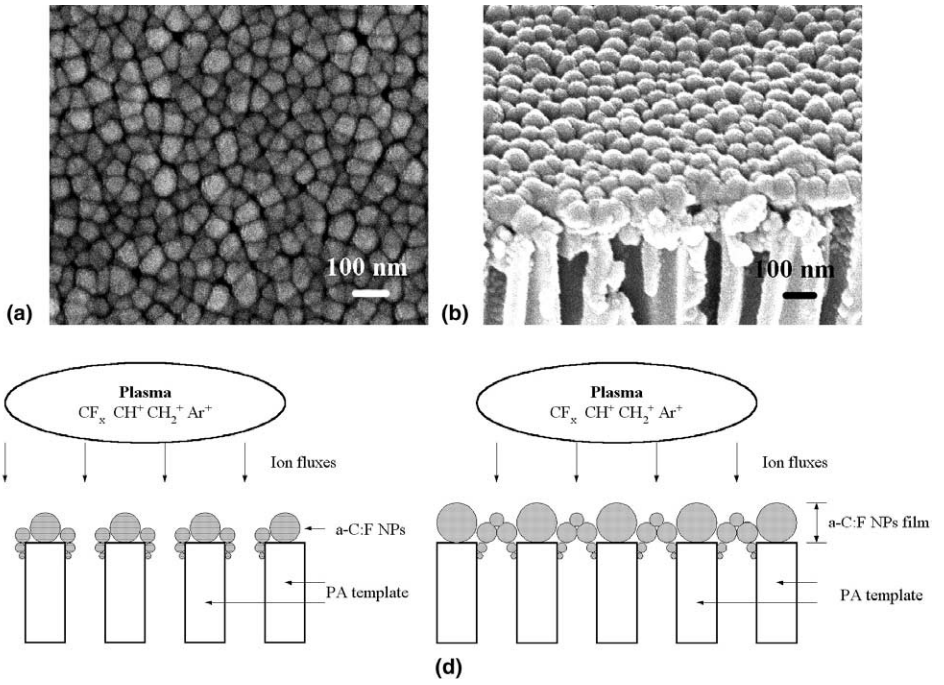

Fig. 1. FESEM image of the a-C:F NPs films, showing: (a) surface morphology and (b) the cross-sectional view. Schematic of the growth mechanism of a-C:F NPs films, (c) initial stage and (d) final stage.

tents. The surface compositions (F/C) were determined by the area ratio of C 1s and F 1s XPS spectra, corrected by the atomic sensitivity factors (ASF; C: 0.296 and F: 1). In the C 1s spectra, we observed the C–F and C–F_2 binding at 288.7 and 291.2 eV, respectively, for the film with 10.6 at.% F. The peak observed at 288.7 eV are ascribed to sp^3-hybridized carbon atoms with covalent C–F bonds, which are similar to those in the covalent graphite fluoride compounds, $(CF)_n$ and $(C_2F)_n$. In the F 1s spectra, the peaks are at 687 and 689 eV for the film with 4.2 and 10.6 at.% F, respectively. The peak at 687 eV is assigned to semi-ionic fluorine and 689 eV is close to covalent fluorine. It should be noted that higher CF_4 and lower C_2H_2 flow rate lead to a relative increase of the intensity of C–F_x bonding when the fluorine content increases, and the C 1s and F 1s peaks shift to the higher binding energy side and their intensities become stronger.

In addition to the chemical analysis performed by XPS, Raman spectroscopy was employed to survey the C–C structural modifications. The Raman spectra present two partially overlapping bands characteristic of all a-C films. They usually referred as the D (disorder) and the G (graphite) bands, since they recall more or less close to the Raman spectrum of polycrystalline graphite [11] as well as other forms of non-crystalline graphitic materials [12]. Two Raman spectra obtained from the different fluorine content of the deposited films are shown in Fig. 3. The lower spectrum is typical of a diamond-like film, while the upper one, obtained from a film with 10.6 at.% F, presents a strong luminescence background, characteristic of a polymer-like material. The first band, centered at approximately 1350 cm^{-1}, corresponds to the so-called D-band and is associated with disorder-allowed zone edge modes of graphite that become Raman active due to the lack of long-range order [11]. The second one, which peaked at approximately 1580 cm^{-1}, is known as the G-band and is attributed to E_{2g}-symmetry optical modes occurring at the Brillouin-zone center of crystalline

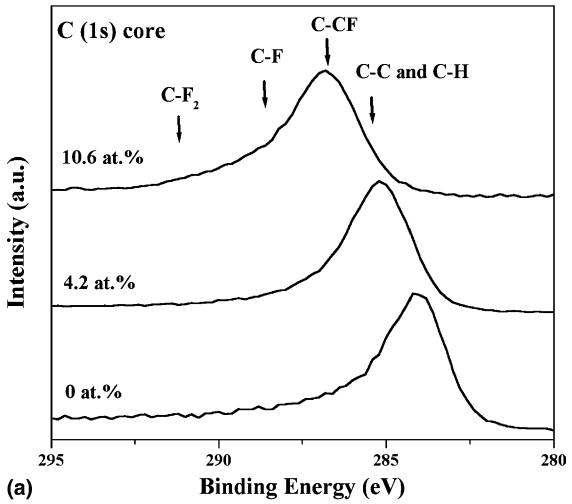

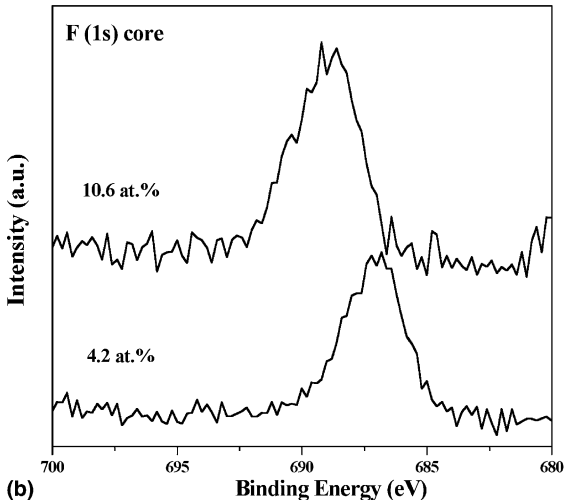

Fig. 2. C (1s) and F (1s) core-level spectra of a-C:F NPs films with different fluorine contents.

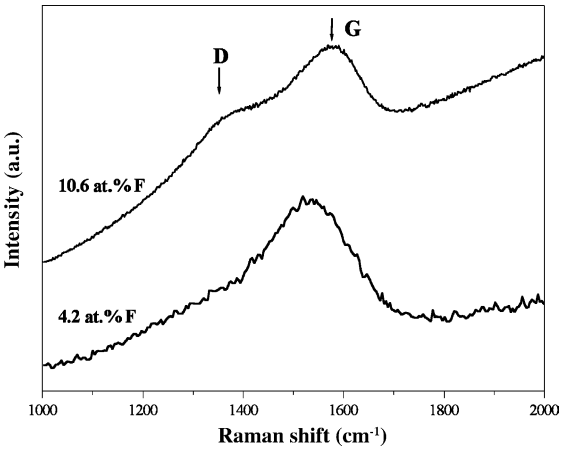

Fig. 3. Raman spectra of a-C:F NPs films.

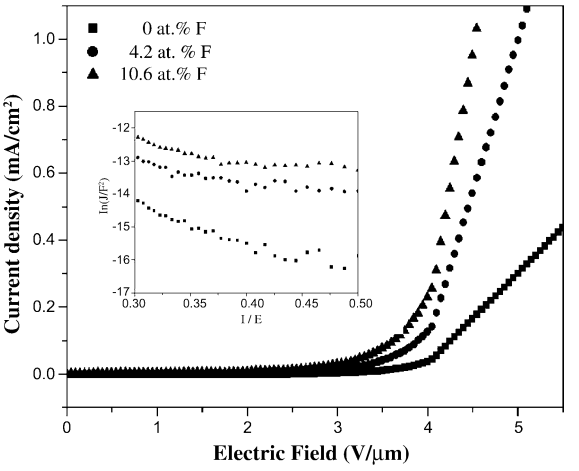

Fig. 4. The *J–E* curves and its Fowler–Nordheim (F–N) plots of the a-C:F NPs films.

graphite [11]. No other band was observed in our a-C:F NPs films.

The *J–E* curves and its Fowler–Nordheim (F–N) plots for the a-C:F NPs films are shown in Fig. 4. Here, we define the turn-on field (E_{to}) as the field needed to produce an emission current density of 10 μA/cm^2. The turn-on fields of the a-C:F NPs films are 3.45 V/μm (0% F), 2.75 V/μm (4.2% F) and 2.25 V/μm (10.6% F). The turn-on field of the fluorinated samples is lower than that of the unfluorinated one. For the conventional flat-panel displays, a current density of 1 mA/cm^2 is usually required. The threshold fields (E_{th}) producing a current density of 1 mA/cm^2 are 7 V/μm (0% F), 5.05 V/μm (4.2% F) and 4.55 V/μm (10.6% F) for the a-C:F NPs films. From the results, the unfluorinated samples need a higher field to emit the electron than fluorinated ones. It should be noted that the emission current density is of the order of 0.5 mA/cm^2 without large fluctuations for a test period of 4 h. Then the samples were taken out to observe the changes of the morphology. The morphology of a-C:F NPs films have no apparent

changes and are not destroyed after the electron field-emission measurements and the field-emission properties of the films are excellent compared with a-C [2,13] and CNTs [14,15].

The reason why a lower field is required to emit electrons from a-C:F NPs films is explained as follows: (1) *The shape effect*: the end of a nanotube is a cap consisting of pentagons and hexagons. The curve position of the nanotube consists of pentagons, hexagons and heptagons. The pentagons and heptagons are considered defects as compared with the hexagons. It is known that the defects are the possible emission sites. It is observed from the SEM images that the a-C:F NPs are irregular spheres and the surface of which is ragged. The nanoparticle has more defects than normal, straight nanotube in a unit area, i.e., the nanoparticle has more possible emission sites than the nanotube. Therefore, we attributed the low turn-on field of a-C:F NPs films to the shape effect [5]. (2) *The donor effect*: the nitrogenation of a-C:H has been investigated and the nitrogen acts an n-type dopant in a-C [16]. A model based on the a-C:H:N (nitrogen containing hydrogenated amorphous carbon) film acting as a 'space charge interlayer' with a lower electron affinity is proposed to explain the emission at lower electric fields than a-C:H [2]. The fluorinated carbon film has more electrons can be emitted than the nitrogenated one when the electric field is applied, because the electronegativity of F atom is higher than N atom. (3) *The dangling bonding effect*: by theoretical calculation, the open end of CNTs with dangling bonds is predicted to be the most favorable structure for field emission [17]. Robertson [18] proposed an emission mechanism for diamond-like carbon films based on the non-uniform hydrogen termination on the film surface. The higher CF_4 concentration, the greater is the probability for the formation of the fluorinated film due to the agglomeration of CF_x radicals [19], but when only CF_4 reactive gas, there is no formation of the fluorinated film. Fluorine atoms can react with hydrogen atoms that are from the hydrocabon radicals on the surface, forming volatile HF and leaving dangling bonds on the film surface [20]. When the fluorine concentration of the a-C:F NPs films increases, more dangling bonds are created on the film surface, which can influence the electronic properties of a-C:F NPs films. The dangling bonds are more reactive and the foreign atoms or molecules may be adsorbed when the samples are exposed to the atmosphere. By an extremely strong local field during the emission process, the attached atoms or molecules may be desorbed, and the dangling bonds may be exposed to contribute greatly to electron emission.

4. Conclusions

In this Letter, a-C:F NPs films with three different fluorine contents were deposited on PA template by an ECR-CVD system. When the fluorine content of the a-C:F NPs films increases, the C 1s and F 1s peaks shift to the higher binding energy side and their intensities become stronger and the microstructure changes from diamond-like film to polymer-like one. From our results, a-C:F NPs films are excellent field emitters compared with a-C and CNTs. The excellent field-emission properties of a-C:F NPs films are due to the effect of the shape, fluorine doping and dangling bonds.

Acknowledgements

The authors acknowledge the financial support of this work by the National Science Council of the Republic of China under the contract of NSC 91-2120-E-007-006.

References

[1] M.W. Geis, J.C. Twichell, J. Macaulay, K. Okano, Appl. Phys. Lett. 67 (1995) 1328.
[2] G.A.J. Amaratunga, S.R.P. Silva, Appl. Phys. Lett. 68 (1996) 2529.
[3] A.G. Rinzler, J.H. Hafner, P. Nikolaev, L. Lou, S.G. Kim, D. Tomanek, P. Nordlander, D.T. Colbert, R.E. Smalley, Science 269 (1995) 1550.
[4] W.A. de Heer, A. Chatelain, D. Ugrate, Science 270 (1995) 1179.
[5] J. Yu, E.G. Wang, X.D. Bai, Appl. Phys. Lett. 78 (2001) 2226.
[6] C.A. Huber, T.E. Huber, M. Sadoqi, J.A. Lubin, S. Manalis, C.B. Prater, Science 263 (1994) 800.

[7] C.R. Martin, Science 266 (1994) 1961.
[8] Z.H. Yuan, H. Hung, H.Y. Dang, J.E. Cao, B.H. Hu, S.S. Fan, Appl. Phys. Lett. 78 (2001) 3127.
[9] S.H. Tsai, F.K. Chiang, T.G. Tsai, F.S. Shieu, H.C. Shih, Thin Solid Films 366 (2000) 11.
[10] X.W. Liu, S.H. Tsai, L.H. Lee, M.X. Yang, A.C.M. Yang, I.N. Lin, H.C. Shih, J. Vac. Sci. Technol. B 18 (2000) 1840.
[11] F. Tuinstra, J.L. Koenig, J. Chem. Phys. 53 (1970) 1126.
[12] D.S. Knight, W.B. White, J. Mater. Res. 4 (1989) 385.
[13] S.R.P. Silva, G.A.J. Amaratunga, J.R. Barnes, Appl. Phys. Lett. 71 (1997) 1477.
[14] P.G. Collins, A. Zettl, Appl. Phys. Lett. 69 (1996) 1969.
[15] X. Xu, G.R. Brandes, Appl. Phys. Lett. 74 (1999) 2549.
[16] S.R.P. Silva, G.A.J. Amaratunga, Thin Solid Films 270 (1995) 194.
[17] S. Han, J. Ihm, Phys. Rev. B 61 (2000) 9986.
[18] J. Robertson, Proc. IVMC'98 (1998) 162.
[19] W. Schwarzenbach, G. Cunge, J.P. Booth, J. Appl. Phys. 85 (1999) 7562.
[20] K. Teii, M. Hori, T. Goto, N. Ishii, J. Vac. Sci. Technol. A 18 (2000) 1.